$N=126$. Large deformations have again appeared near $N=140$. The ratio $(\beta_E/\beta_\tau)^2$ increases from a value of ~ 4.9 at $N=90$ to a value of $\sim 6.5-7$ for $N=108$ to 118. The exact value of $(\beta_E/\beta_\tau)^2$ depends upon the value chosen for the nuclear radius, since the moment of inertia is proportional to $R_0^2\beta^2$ while Q_0^2 is proportional to $R_0^4\beta^2$. However, any reasonable adjustment of the nuclear radius does not remove the discrepancy. The shoulder on both curves, beginning near $N=100$, may be associated with the filling of $i_{13/2}$ neutron orbits.

The large discrepancy between the absolute values of β_E^2 and β_τ^2 is especially interesting. β_E^2 is essentially a measure of mass deformation while β_τ^2 is a measure of charge deformation *of the quadrupole type*. While quadrupole deformation is expected to be the most important type, a nuclear deformation involving higher multipoles could increase the moment of inertia without contributing to quadrupole transition probabilities. A possible consequence of an appreciable octupole deformation is an enhanced $E3$ transition probability. Such $E3$ transitions have not as yet been experimentally observed in this region of the periodic table. Other possible factors which may contribute to the discrepancy have been discussed by Ford.[18]

Any essential difference between the deformation properties of the neutron structure and the proton structure will lead to different values of β_E^2 and β_τ^2. If such differences exist, they might be best revealed through measurements of the gyromagnetic ratio, since the gyromagnetic ratio of the core depends upon the particular manner in which angular momentum is distributed among the constituents of the core. A breakdown of the assumption of irrotational flow can of course explain the observed large moments of inertia.

We would like to express our appreciation to Dr. M. Goldhaber and Dr. J. Weneser for several interesting discussions, to R. L. Chase and W. Higginbotham for advice in equipment design, and to Dr. D. E. Alburger, Dr. E. L. Church, and Dr. J. W. Mihelich for making certain radioactive sources available to us.

PHYSICAL REVIEW VOLUME 98, NUMBER 3 MAY 1, 1955

Low-Energy Protons from Targets Bombarded by 15-Mev Deuterons*

F. A. ASCHENBRENNER†

Physics Department and Laboratory for Nuclear Science, Massachusetts Institute of Technology, Cambridge, Massachusetts

(Received December 6, 1954)

A particle-selection technique is described which makes it possible to identify readily the reaction particles from deuteron-induced reactions. The results of a study of the low-energy protons from targets bombarded by 15-Mev deuterons is presented. The proton energy spectra from niobium, silver, antimony, tantalum, three lead isotopes, and uranium bombarded with the direct deuteron beam were observed at several angles. In addition, the proton energy spectrum from tantalum was observed at several deuteron beam energies ranging from approximately 10.5 to 15 Mev. The low-energy parts of the proton spectra show what appears to be a Coulomb barrier effect. However, protons are observed several Mev below the Coulomb barrier for protons, indicating that the barrier effect differs from the ordinary Coulomb barrier penetration of protons emerging from a compound nucleus. The behavior of the barrier effect with respect to changes in counter angle, Z (atomic number), and A (mass number) of the targets, and deuteron beam energy was observed.

I. INTRODUCTION

WHEN thin targets are bombarded with deuterons, several types of particles are emitted. Of these, protons and neutrons have been found to be the most abundant. In general, the yield for deuteron-induced reactions is much larger than that of corresponding reactions with other charged particles. For this reason, deuterons are commonly accelerated in cyclotrons for the purpose of radioactive isotope production.

In recent years (d,p) reactions have been subjected to large numbers of experimental and theoretical investigations. In general these investigations have been conducted for two purposes. These are: (1) A study of the properties of the energy levels of the residual nuclei through observations of the proton energy groups; (2) A study of the mechanism of the (d,p) reaction.

Symbolically, the (d,p) reaction can be written:

$$X+d\rightarrow Y+p+Q,$$

where X is the target nucleus; Y is the residual nucleus; and Q is the reaction energy balance, commonly called the Q of the reaction. For a Q greater than -2.23 Mev (where 2.23 Mev is taken to be the binding energy of the deuteron), the residual nucleus is stable against neutron emission and in general, against any heavy-particle emission. For Q less than or equal to -2.23 Mev, sufficient energy has been transferred to the

* Submitted to the Department of Physics, Massachusetts Institute of Technology in partial fulfillment of the requirements for the degree of Doctor of Philosophy. This work has been supported in part by the joint program of the Office of Naval Research and the U. S. Atomic Energy Commission.

† Now at the ANP Department of the General Electric Company, Cincinnati, Ohio.

residual nucleus to allow neutron emission. In this case the reaction can be written:

$$X+d\rightarrow Y+p+Q\rightarrow(X+n)+p+Q.$$

It is obvious that for $Q=-2.23$ Mev sufficient energy has been supplied by the kinetic energy of the deuteron to separate the proton and neutron in the deuteron.

For the cases when neutron emission is possible (Q less than -2.23 Mev) the energy-level widths are much larger than for the cases when neutron emission is not possible. Except for very light nuclei, the level widths when neutron emission is possible are greater than the level separations. Therefore, observation of the proton spectra for Q less than -2.23 Mev in heavy nuclei gives information on level densities rather than on discrete energy levels. This region is generally referred to as a continuum.

The (d,p) reactions with Q greater than -2.23 Mev can occur in two possible ways. The first possibility is for the deuteron to enter the nucleus as a unit, forming a compound nucleus, with the subsequent emission of a proton. The very high cross sections observed with low deuteron bombarding energies could not be explained by this picture, in which the deuterons were required to penetrate the Coulomb barrier. In order to explain these high cross sections, Oppenheimer and Phillips[1] proposed that the deuteron is polarized in the Coulomb field of the nucleus and the neutron is captured without the proton entering the nucleus. Later, Peaslee[2] concluded that the compound-nucleus formation is less important than the Oppenheimer-Phillips, or stripping, reaction at all deuteron bombarding energies. Peaslee formulated a semiclassical theory that is in agreement with observed (d,p) excitation functions.

More recently, a wave-mechanical description of the (d,p) stripping reaction was formulated by Butler[3] which neglected Coulomb effects. The agreement between experimental data[4] and Butler's formulation, in which the neutron is captured by the target nucleus, has made it possible to determine the orbital quantum number of the captured neutron in many cases.

The protons with energies corresponding to (d,p) reactions with Q less than -2.23 Mev can result from another process. This is the electric breakup of the deuteron by the Coulomb field of the nucleus. Cross sections for the electric breakup process have been calculated by Guth and Mullin[5] to be of the order of 200 millibarns for targets of Z greater than 29 bombarded with 15-Mev deuterons. This would predict a strong competition between the electric breakup process and (d,p) stripping.

The development of a convenient particle-selection technique at the M. I. T. cyclotron has made it possible to study the entire proton spectra from targets with Z greater than 41. A study of the low-energy protons from selected targets bombarded with the M. I. T. cyclotron deuteron beam has been conducted to determine what processes are most important in producing the low-energy protons.

II. EXPERIMENTAL PROCEDURE

A. Cyclotron and Emergent Beam

The source of high-energy deuterons used for these experiments has been the M. I. T. cyclotron, which produces an external beam of approximately 15 Mev.[6] The scattering chamber is connected to the cyclotron with a tube through which the deuterons are conducted. The tube contains several tantalum baffles to prevent the target from seeing small-angle scattered deuterons. A defining aperture is placed at the entrance of the scattering chamber. The deuterons are focused on the target at the center of the scattering chamber with a focus magnet that is located in the cyclotron vault. The focusing system produces a spot on the target that is approximately $\frac{1}{4}$ inch wide and $\frac{3}{8}$ inch high.

For some of the experiments, a foil changer was placed between the conducting tube and the scattering chamber. This foil changer made it possible to insert aluminum foils in the deuteron beam to reduce the beam energy at the target.

The scattering chamber has been previously described by Harvey.[7]

B. Particle-Selection Technique

A convenient method for identifying the charged particles from deuteron induced reactions has been found to be a simultaneous determination of the energy and the initial specific ionization of each reaction particle. For this purpose two scintillation counters are used (Fig. 1). The first is a thin plastic scintillation counter which measures the initial specific ionization of the reaction particles. The second is a NaI(Tl) scintillation counter which measures the remaining

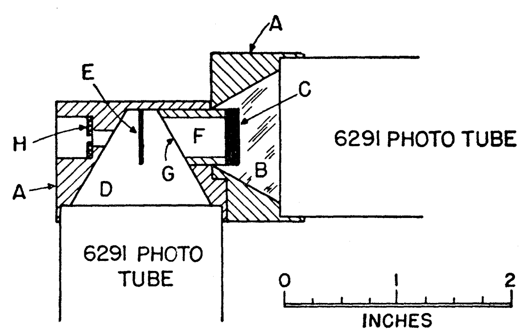

FIG. 1. Schematic diagram of particle selective counter. *A*—Aluminum; *B*—Lucite; *C*—NaI(Tl); *D*—space; *E*—plastic scintillator; *F*—aluminum cylinder; *G*—aluminum foil; *H*—lead.

[1] J. R. Oppenheimer and M. Phillips, Phys. Rev. **48**, 500 (1935).
[2] D. C. Peaslee, Phys. Rev. **74**, 1001 (1948).
[3] S. T. Butler, Proc. Phys. Soc. (London) **208**, 559 (1951).
[4] C. F. Black, Ph.D. thesis, Massachusetts Institute of Technology, February 1953 (unpublished).
[5] C. J. Mullin and E. Guth, Phys. Rev. **82**, 141 (1951).
[6] M. S. Livingston, J. Appl. Phys. **15**, 2 (1944).
[7] J. A. Harvey, Phys. Rev. **81**, 353 (1951).

energy of the reaction particles after they pass through the thin counter. The combined information from these counters makes it possible to identify protons, deuterons, tritons, and alpha particles with ranges large enough to pass through the first counter and strike the NaI(Tl) crystal.

Calculations from range-energy curves show that protons, deuterons, and tritons with equal incident energies lose amounts of energy in the plastic scintillator in the 1:1.8:2.6. However, since plastic scintillators have a nonlinear response for particles of high dE/dx (similar to stilbene and anthracene[8]), the ratios of the pulses for these particles coming from the thin counter deviate from the calculated ratios. The deviations depend upon the incident energies. Because the information from the thin counter is used only to identify the reaction particles, these deviations are serious only at the lower part of the energy spectrum.

During most of the experiments, a 28-mg/cm² thick Pilot scintillator B was used in the first counter.[9] The scintillator was machined to this thickness from a larger piece with a machine-shop lathe. The resolution obtained for 15-Mev deuterons scattered 45° elastically with a thin gold foil was 13 percent. In this case, the deuterons lost approximately 2 Mev in the plastic scintillator.

Separated particle energy groups can readily be identified and measured using an oscilloscope display system in conjunction with the counter combination. The procedure that can be used is as follows:

The output pulses from the two scintillation counters are shaped so that they have flat tops, and then they are displayed on the two axes of an oscilloscope. The pulses from each of the scintillation counters are also sent through two very stable single-channel analyzers and a coincident circuit. The coincident in time is used to trigger a Schmitt trigger circuit whose output pulse is applied to the intensity grid of the oscilloscope. The delay of the coincident pulse is arranged so that it intensifies the beam of the oscilloscope only when the pulses displayed on the two axes are at their maxima. This results in a small spot appearing on the screen of the oscilloscope. The position of this spot shows the amplitudes of the two pulses coming from the two counters.

Figure 2(a) shows a time-exposure photograph of the oscilloscope screen with the particle selective counter observing the reaction particles from a $C^{12}+H^1$ target bombarded with 15-Mev deuterons at an angle of 30° from the incident deuteron beam. Figure 2(b) shows the same thing when a partially oxidized Be^9 target is observed at an angle of 35° from the incident deuteron beam. In both cases the pulses from the thin plastic scintillation counter (E_1) are displayed on the X-axis

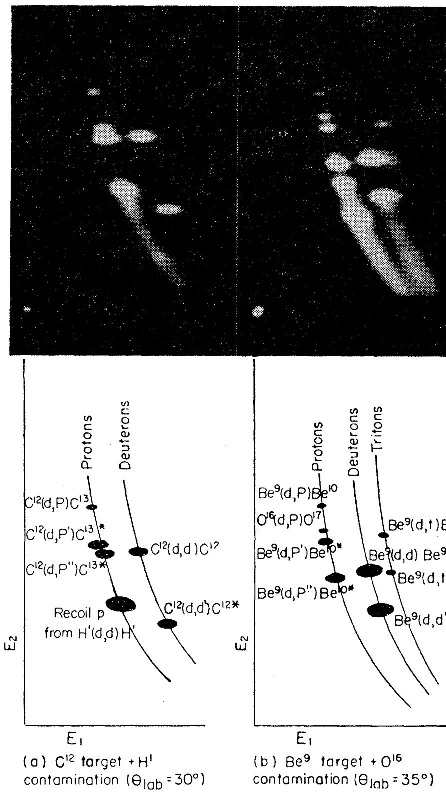

FIG. 2. Time exposure photographs of the oscilloscope screen with the particle selective counter observing reaction particles from 15-Mev deuteron induced reactions. Pulses from the thin plastic scintillation counter (E_1) are displayed on the X-axis and the pulses from the NaI(Tl) counter (E_2) are displayed on the Y-axis. Reprinted in part from M. I. T. Laboratory for Nuclear Science, Progress Report (August 31, 1953).

and the pulses from the NaI(Tl) counter (E_2) are displayed on the Y-axis. In the photographs several particle energy groups can be observed. Included in Fig. 2 are sketches showing the identification of some of the groups. For the groups that are well separated, one can visually adjust the bias and window width of each of the single channel analyzers so that only the spot corresponding to the group desired remains on the oscilloscope screen. The intensity of this group can then be measured by feeding the coincidence pulses into a scaler.

There is a theoretical quantum-mechanical relationship which predicts dE/dx caused by collision processes. As given by Livingston and Bethe,[10] this relationship is

$$(dE/dx)_c = -(4\pi e^2 z^2 N/mv^2)\{Z[\log_e(2mv^2/I) - \log_e(1-v^2/c^2) - v^2/c^2] - C_k\},$$

where z is the charge of the particles, v is the velocity of the particles, e is the charge on the electron, m is the mass of the electron, N is the atomic density of the

[8] Taylor, Jentschke, Remley, Eby, and Kruger, Phys. Rev. 84, 1034 (1951).

[9] The plastic scintillator was obtained from Pilot Chemicals, Inc., 47 Felton Street, Waltham, Massachusetts.

[10] M. S. Livingston and H. A. Bethe, Revs. Modern Phys. 1, 263 (1937).

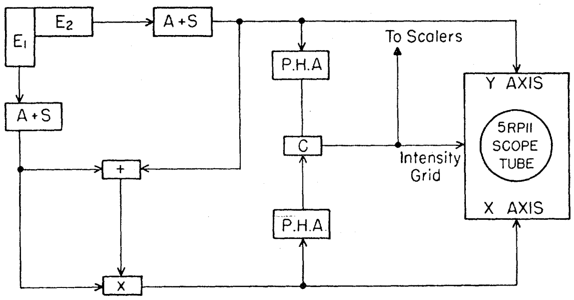

FIG. 3. Block diagram showing the arrangement of the electronic apparatus. E_1—Thin plastic scintillation counter; E_2—NaI(Tl) scintillation counter; $A+S$—pulse amplifier and shaper; P.H.A —pulse height analyzer; X—pulse multiplier; $+$—pulse adder; C—coincidence circuit.

absorber, Z is the effective nuclear charge of the absorber, I is the effective ionization potential of the absorber, c is the velocity of light, and C_k is a correction term unimportant at high speeds. For nonrelativistic particles, the above expression reduces to

$$(dE/dx)_e = Kz^2/v^2,$$

where K varies only slightly with energy. Thus, the product $E(dE/dx)$ for nonrelativistic particles is approximately Cz^2M, where C is a constant and M is the mass.

In the case of the particle selective counter, the particles lose an appreciable amount of energy in the plastic scintillator which is used to measure dE/dx. Therefore, the product $E_1 \cdot E_2$, where E_1 is the energy loss in the plastic scintillator and E_2 is the energy loss in the NaI(Tl) crystal, is not proportional to z^2M. Calculations from range-energy curves show that the product $E \cdot E_1$, where $E = E_1 + E_2$, is a constant proportional to the mass for protons in the region 5 to 20 Mev, for deuterons in the region 7 to 20 Mev, and for tritons in the region 9 to 20 Mev. The products for protons, deuterons, and tritons have ratios 1:1.8:2.6.

Figure 3 shows a block diagram of the electronic apparatus used when the product $E \cdot E_1$ is used to identify the reaction particles. The pulses from the two scintillation counters are first added electronically and then fed into one input of the pulse multiplier,[11,12] while at the same time the pulses from the plastic scintillation counter are fed into the other input. The output from the pulse multiplier is then displayed on the X-axis of the oscilloscope, and the output from the NaI(Tl) scintillation counter is displayed on the Y-axis. The relative gains of the pulse amplifiers are then adjusted to make the protons appear on a straight line. Figure 4(a) is a time-exposure photograph of the oscilloscope screen with the particle selective counter observing the reaction particles from the oxidized Be^9 target bombarded with 15-Mev deuterons at an angle of 45 degrees from the incident deuteron beam. The deviation of the deuteron spots from a straight line is believed to be due to the nonlinear response of the plastic scintillator to particles of high dE/dx. In the photograph the elastic deuteron group appears to be a doublet. That is because the center-of-mass effect causes the elastic deuterons from Be^9 to have lower energies than those from O^{16}.

The advantage of using the product $E \cdot E_1$ to identify the reaction particles is that a large part of the energy spectrum can be observed with the E_2 pulse-height analyzer while using only one adjustment of the product analyzer. This is demonstrated in Figs. 4(b) and 4(c).

When bombarding targets of high atomic number, no low-energy deuterons are observed. In these cases, a pulse-height analysis of the entire proton energy spectrum can be made using only one adjustment of the product analyzer. Figure 5 shows one example. Figure 5(b) shows all the reaction particles emitted at 90 degrees when Pb^{206} is bombarded with 15-Mev deuterons. Figure 5(a) shows the same thing when the bias and window width of the product analyzer is adjusted to count only protons.

The human eye does not integrate well the light flashes on the oscilloscope screen. Therefore, time-exposure photographs of the oscilloscope screen are made with a Polaroid Land Camera to determine whether or not the visual adjustments of the amplifier gains and the analyzer bias and window widths are correct.

C. Beam Energy Measurement and Energy Calibration

To determine the deuteron beam energy a 0.002-inch thick polyethylene target is inserted in the beam at the center of the scattering chamber. A scintillation spectrometer is used to observe the energy spectrum of the protons after they pass through a 217.7-mg/cm^2 thick aluminum absorber at an angle of 45 degrees from the

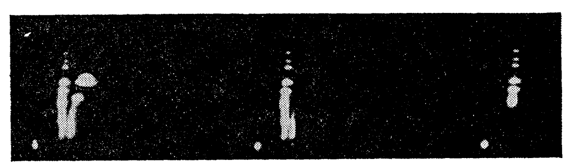

(a) (b) (c)

FIG. 4. Photograph of oscilloscope screen when counter is observing oxidized Be target at 45 degrees from the incident deuteron beam. Beam energy is approximately 15 Mev. Multiplier output is displayed on X-axis and E_2 is displayed on Y-axis. (a) Analyzers adjusted to count all particles. (b) Product analyzer adjusted to count protons. Some low-energy deuterons are leaking through. (c) Analyzers adjusted to count only protons. This shows the part of the proton spectrum that can be measured with only one adjustment of the product analyzer.

[11] The multiplier circuit is a slight extension of a multiplier designed by C. W. Johnstone of Los Alamos, having a 5×5 array of 6BN6 tubes for multiplying instead of the 3×4 originally used by Johnstone. The use of the 5×5 array was suggested by Johnstone.

[12] F. A. Aschenbrenner, M. I. T. Laboratory for Nuclear Science, Progress Report, August 31, 1953 (unpublished).

(a) (b)

FIG. 5. Photograph of oscilloscope screen when counter is observing Pb^{206} target bombarded with 15-Mev deuterons. Multiplier output displayed on X-axis, E_2 displayed on Y-axis. Counter angle 90 degrees. (a) Product analyzer adjusted for protons. (b) Analyzers adjusted for all particles.

incident deuteron beam. The ratio E_p/E_p' where E_p and E_p' are the energies of the protons incident on the NaI(Tl) crystal from the reactions $C^{12}(d,p)C^{13}$ and $C^{12}(d,p')C^{13*}$, is determined by measuring the positions of the two highest-energy proton groups. Since E_p and E_p' depend upon the energy of the incident deuterons, the ratio E_p/E_p' can be used to determine the deuteron beam energy.

After the deuteron beam energy is determined, the proton energy from the reaction $C^{12}(d,p)C^{13}$ is calculated; then with the help of range-energy curves, the energy of this proton group in the second counter (E_2) of the particle selective counter is determined. The position of the peak is also measured with the particle selective counter, which then determines E_2 as a function of pulse height. After the E_2 spectrum of protons from an unknown target is measured with the particle selective counter, range-energy curves are consulted to determine the corresponding energies of the protons coming from the center of the target.

D. Cross-Section Measurements

The beam monitor consists of a scintillation spectrometer which is mounted so that it observes particles scattered 45 degrees from the incident deuteron beam by a thin gold foil. The bias and window width of the monitor differential discriminator were adjusted so that it accepted only those pulses which were due to the particles with energy in the vicinity of the elastic deuterons. For incident deuteron beam energies between 10 and 15 Mev, over 97 percent of these particles are elastic deuterons. Previous measurements of these cross sections agree within 10 percent with the cross sections calculated for Rutherford scattering.[13]

Since the beam monitor does not measure directly the deuteron beam, the differential cross sections were measured relative to a differential cross section that has been previously measured by three independent methods. This cross section is for protons from the reaction $Ta^{181}(d,p)Ta^{182}$ with Q greater than -2.32 Mev at 90 degrees from a 14-Mev deuteron beam.[14] The differential cross sections can readily be expressed in terms of this standard:

$$\sigma=\frac{C/N}{C_s/N_s}\,\frac{A/T}{A_s/T_s}\,\frac{\cos\phi}{\cos\phi_s}\,\sigma_s,$$

where σ = differential cross section in mb/atom·steradian in the laboratory system, C = integral counts or area under the differential spectrum curve, N = number of incident deuterons, A = atomic weight of target, T = thickness of target, ϕ = angle normal of target makes with deuteron beam, and s = subscript denoting the same value for the standard measurement. Assuming that the monitor counts only elastically scattered deuterons, then $N\propto M/\Omega\sigma_e$, where M is the number of monitor counts, Ω is the monitor counter solid angle, and σ_e is the differential cross section for elastic deuterons. Assuming further that the differential cross section for elastic deuterons is given by the Rutherford cross sections, then; $\sigma_e\propto 1/E_d^2$ or $N\propto ME_d^2/\Omega$ and $N_s\propto ME_d^2/\Omega_s$, where E_d is the deuteron beam energy at the monitor counter.

The deuteron beam energy was reduced to 14 Mev for the standard measurement by inserting aluminum foils in the deuteron beam. Total cross sections were obtained by integrating graphically the angular distributions of the differential cross sections. Since, however, extreme forward angles could not be measured, the values for total cross sections obtained are only approximate values.

E. Experimental Uncertainties

The separation of the protons and deuterons for all the targets observed in this study was quite good. Figure 5 shows one example. The photographs (Fig. 5) give the impression that, with the correct adjustments of the product analyzer bias and window width, clean proton energy spectra are observed. This is a wrong impression. Because of the long resolving time required for the coincident circuit, chance coincidences between γ rays and protons are possible. However, these chance coincidences are appreciable only at the low end of the energy spectrum where the γ-ray intensity is high. It was possible to establish the approximate shape and magnitude of the chance coincidence background by observing the E_2 spectra with a very thin plastic scintillator in the first counter.

The following sources of error effect the beam energy measurement and energy calibration: (1) Error in thickness measurements of plastic scintillators and aluminum foils in the first counter; (2) error in range-energy curves; (3) nonlinear response of NaI(Tl) crystals; (4) error in $C^{12}(d,p)C^{13}$ and $C^{12}(d,p')C^{13*}$ Q-values; (5) error in locating the centers of the $C^{12}(d,p)C^{13}$ and $C^{12}(d,p')C^{13*}$ proton peaks; and (6) incorrect determinations of counter angles and target angles. After careful consideration of all the sources of error, it is estimated that the deuteron beam energies were determined to well within 200 kev, and the proton

[13] H. E. Gove, M. I. T. Laboratory for Nuclear Science and Engineering, Progress Report, July 1, 1950 (unpublished).

[14] Gove, Harvey, Livingston, Boyer, and Zimmerman, M. I. T. Laboratory for Nuclear Science and Engineering, Progress Report, April 1, 1950 (unpublished).

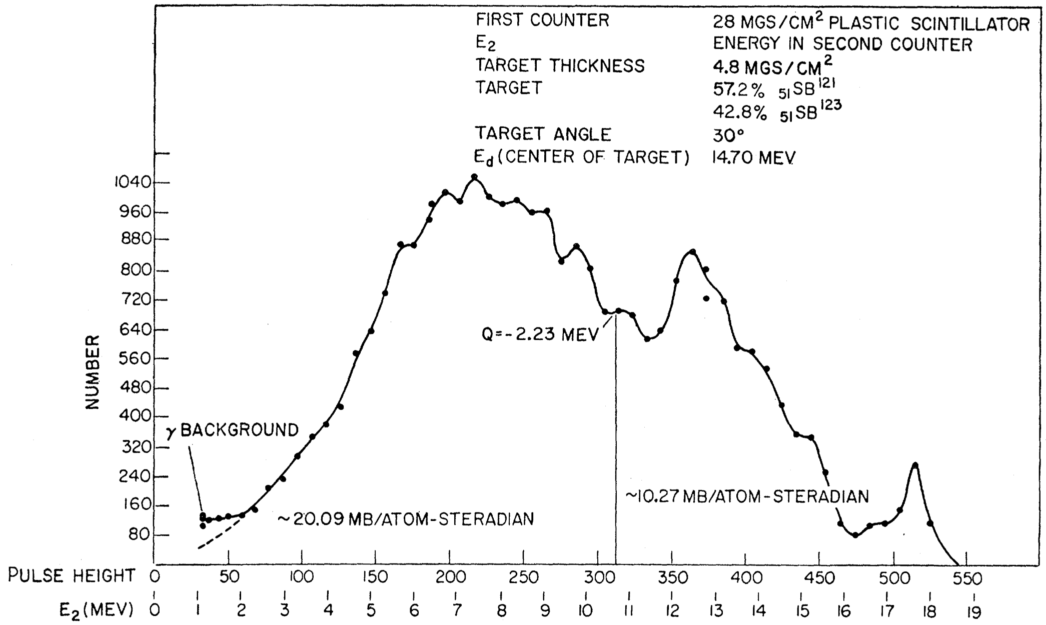

FIG. 6. Energy spectrum of protons from Sb as observed in the second counter. Counter angle 60 degrees. Deuteron beam energy 14.78 Mev.

energy calibrations are estimated to be accurate to within 350 kev. Checks on proton groups with previously measured Q-values indicate that, in most cases, the energy calibrations were considerably better than the values quoted here.

The accuracy of the differential cross sections depend upon the accuracy of target thickness determinations, the extent to which the monitor counter observed Rutherford scattered deuterons, the saturation of the monitor counter caused by high counting rates and the accuracy of the value assumed for the standard. It is estimated that the differential cross sections are correct only to within 20 percent. Since the differential cross sections for extreme forward angles were not measured, the values quoted for the total cross sections can only be considered as rough estimates that are probably

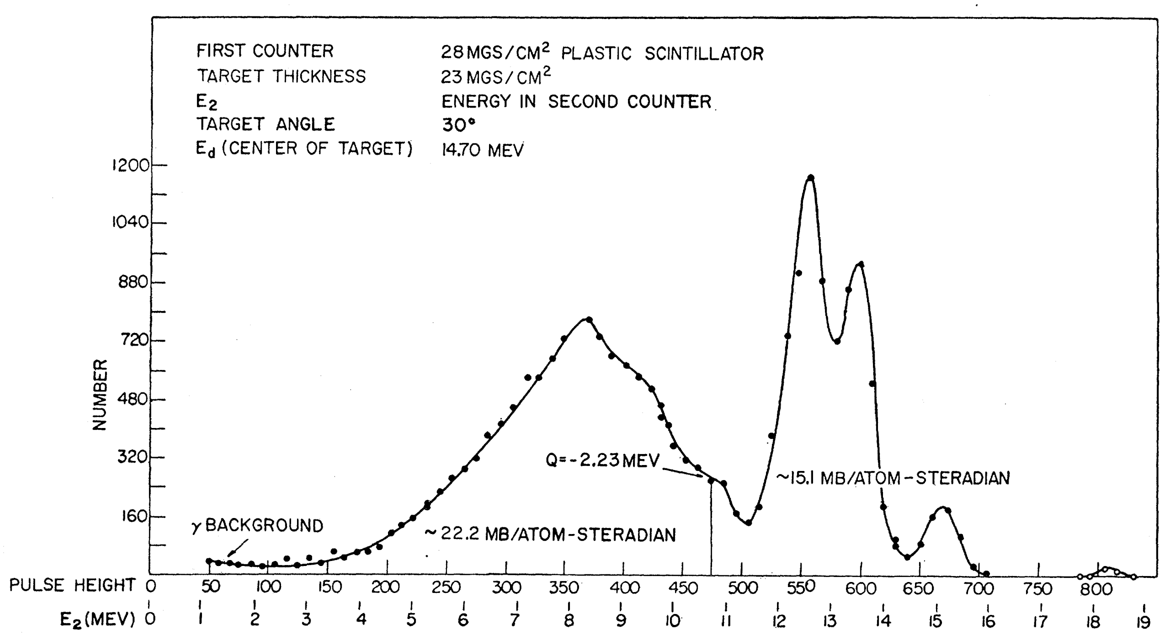

FIG. 7. Energy spectrum of protons from Pb^{207} as observed in the second counter. Counter angle 75 degrees. Deuteron beam energy 14.85 Mev.

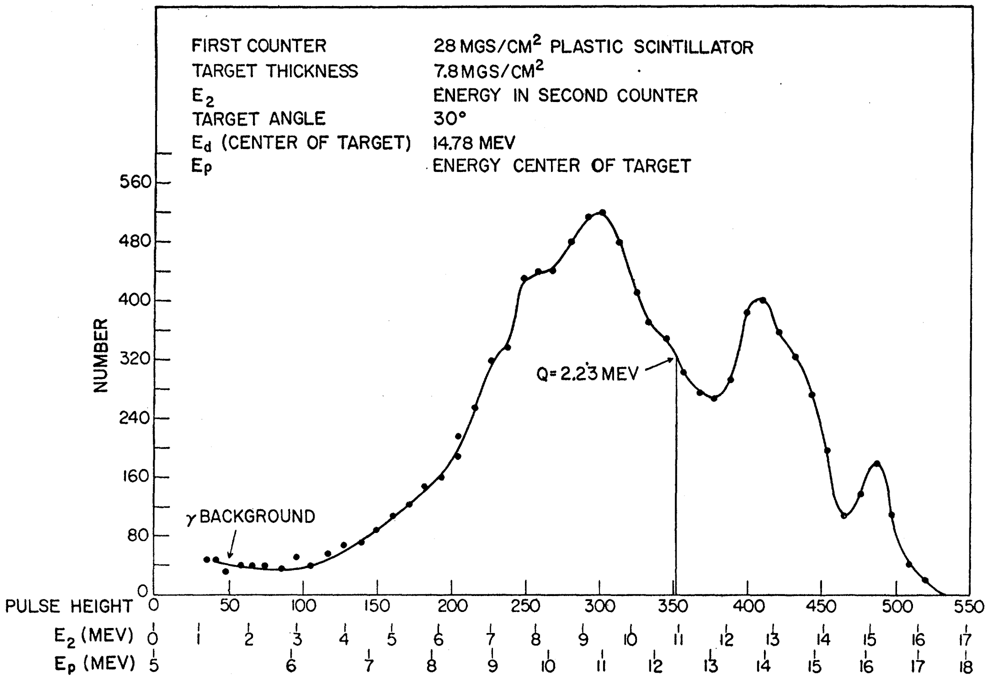

FIG. 8. Energy spectrum of protons from U^{238} as observed in the second counter. Counter angle 90 degrees. Deuteron beam energy 14.82 Mev.

correct to only ± 40 percent, and in some cases they may be less accurate.

III. EXPERIMENTAL RESULTS

The proton energy spectra from niobium, silver, antimony, tantalum, three lead isotopes, and uranium bombarded with the direct deuteron beam were observed at several angles. Figures 6, 7, and 8 show three examples. In addition the proton energy spectrum from tantalum was observed at several deuteron beam energies ranging from approximately 10.5 to 15 Mev. In these experiments, the direct deuteron beam energy was reduced by inserting aluminum foils.

The proton energy spectra were divided into two parts, using Q equal to -2.23 Mev as the dividing line. This division is made because the protons from (d,p) reactions with Q greater than -2.23 Mev leave the residual nucleus in states in which the neutron is bound. The protons for which Q is less than -2.23 Mev leave the residual nucleus in unbounded states, making it possible for the residual nucleus to decay by neutron emission. Proton spectra from (d,p) reactions with Q greater than -2.23 Mev have been previously studied[14] and are included here only for a comparison with the proton spectra for Q less than -2.23 Mev.

In considering the proton spectra with Q less than -2.23 Mev, a broad peak is observed in each case. Superposed on this broad peak is a variation of proton intensity indicating a variation of level density in the residual nucleus, especially between the broad peak and the line for Q equal to -2.23 Mev. For experimental reasons the spectra were not investigated in sufficient detail to establish the exact energy-level structure.

The low-energy parts of the proton spectra show what appears to be a Coulomb barrier effect. It is believed that, if the γ-proton coincidence background was absent, an experimental cutoff would be observed, where "experimental cutoff" is construed to mean that the intensity decreases to a very small fraction of the intensity that could be observed with the experimental

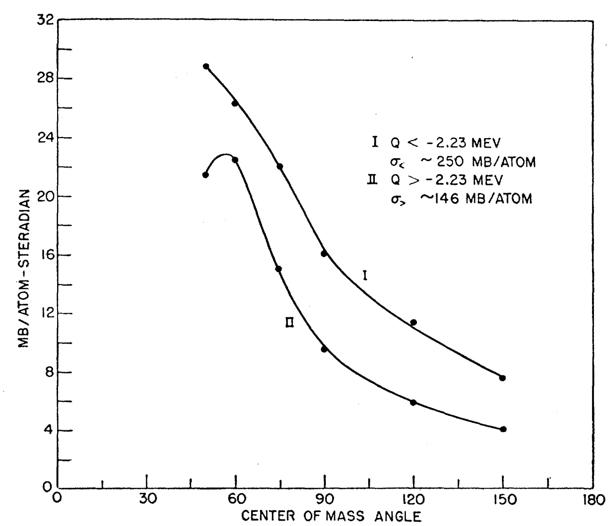

FIG. 9. Angular distribution of protons emitted when Pb^{207} is bombarded with 14.8-Mev deuterons.

Table I. Summary of estimated cross sections and apparent experimental cut-off energies.[a]

Target	E_d Mev	E_d (c.m.) Mev	B Mev	$\sigma_<$ mb	$\sigma_>$ mb	σ_T mb	E_c Mev
$_{92}U^{238}$	14.82	14.53	14.25				6.6
$_{82}Pb^{208}$	14.8	14.35	13.37	230	133	363	6.35
$_{82}Pb^{207}$	14.85	14.42	13.37	250	146	396	6.48
$_{82}Pb^{206}$	14.80	14.37	13.37	227	131	358	6.40
$_{73}Ta^{181}$	14.75	14.24	12.38	240	103	343	5.80
$_{73}Ta^{181}$	13.97	13.47	12.38	299	140	439	5.80
$_{73}Ta^{181}$	12.80	12.32	12.38	276	216	492	5.70
$_{73}Ta^{181}$	11.71	11.25	12.38	228	283	511	5.60
$_{73}Ta^{181}$	10.84	10.35	12.38	183	230	413	5.50
$_{51}Sb^{121,123}$	14.78	14.23	9.87	277	128	405	4.33
$_{47}Ag^{107,109}$	14.94	14.30	9.48	284	100	384	4.20
$_{41}Nb^{93}$	14.89	13.85	8.69				3.50

[a] E_d = deuteron beam energy in laboratory coordinates, E_d(c.m.) = deuteron beam energy in center-of-mass coordinates, B = the Coulomb barrier height, $\sigma_<$ = the estimated cross section for $Q<-2.23$ Mev, $\sigma_>$ = the estimated cross section for $Q>-2.23$ Mev, σ_T = the total cross section, E_c = apparent experimental cut-off energy.

setup. The data curves were extrapolated to zero intensity in order to obtain an estimate of where the experimental cutoff would be. Although it was not definitely established that an experimental cutoff exists, a study of the extrapolated points is justified because it offers a method for studying the slope and position of the Coulomb barrier effect.

The properties of the proton spectra for Q less than -2.23 Mev can be summarized as follows:

(1) In each case a broad peak was observed.

(2) Superposed on the broad peak is a variation of proton intensity, especially between the peak and the line at $Q=-2.23$ Mev.

(3) The angular distribution for all the protons with Q less than -2.23 Mev in each case is peaked forward, and the shape of this angular distribution is very similar to that for Q greater than -2.23 Mev, Fig. 9 shows one example.

(4) The total cross sections for Q less than -2.23 Mev are of the same order of magnitude as for Q greater than -2.23 Mev. (See Table I.)

(5) The low-energy part of each proton spectrum shows what appears to be a Coulomb barrier effect. However, protons are observed several Mev below the Coulomb barrier for protons, indicating that the barrier effect differs from the ordinary Coulomb barrier penetration of protons emerging from a compound nucleus.

(6) An apparent experimental cutoff (E_c) is observed at the low-energy end of the spectrum which has the following properties: (a) E_c is independent of angle within the accuracy of the experiments; (b) E_c is the same for neighboring isotopes within the accuracy of the experiments; (c) E_c varies less than 500 kev from deutron bombarding energies ranging from 10.84 to 14.75 Mev for the one case studied (see Fig. 10 and Table I); (d) E_c increases with increasing barrier height (see Fig. 11 and Table I).

IV. CONCLUSIONS

All the properties noted above appear to be qualitatively consistent with a stripping model in which the deuteron is first polarized and stretched by the Coulomb field, and then the neutron is stripped off leaving the proton outside the Coulomb barrier. Peaslee, using a semiclassical theory for (d,p) stripping, calculated (d,p) excitation functions which show fair agreement with experimental excitation functions.[2] These excitation functions show the same kind of barrier effect as observed in the proton spectra in the present experiments. By extrapolating the excitation functions to zero at low deuteron energies, one can obtain an ap-

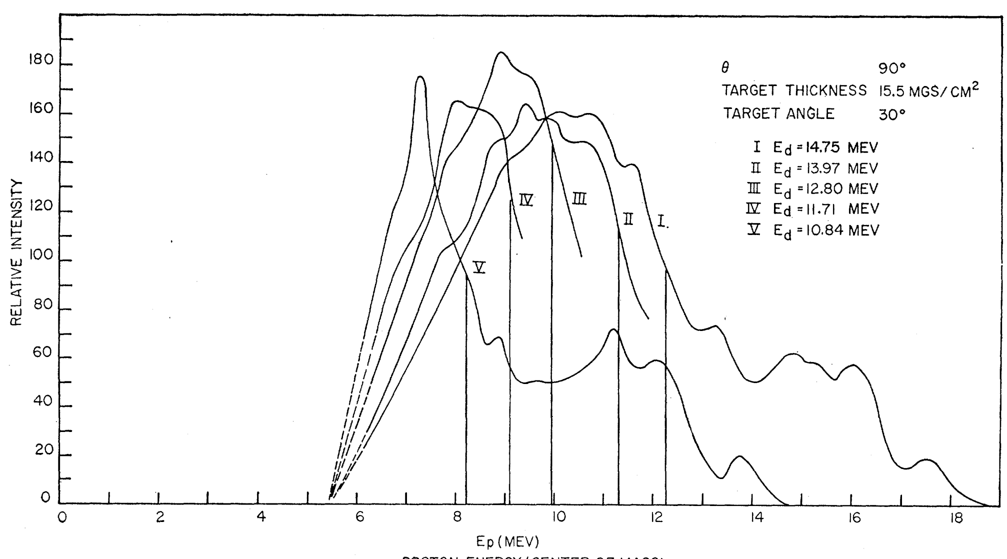

Fig. 10. Variation of low-energy part of proton spectrum with deuteron beam energy. Dashed lines obtained by extrapolation.

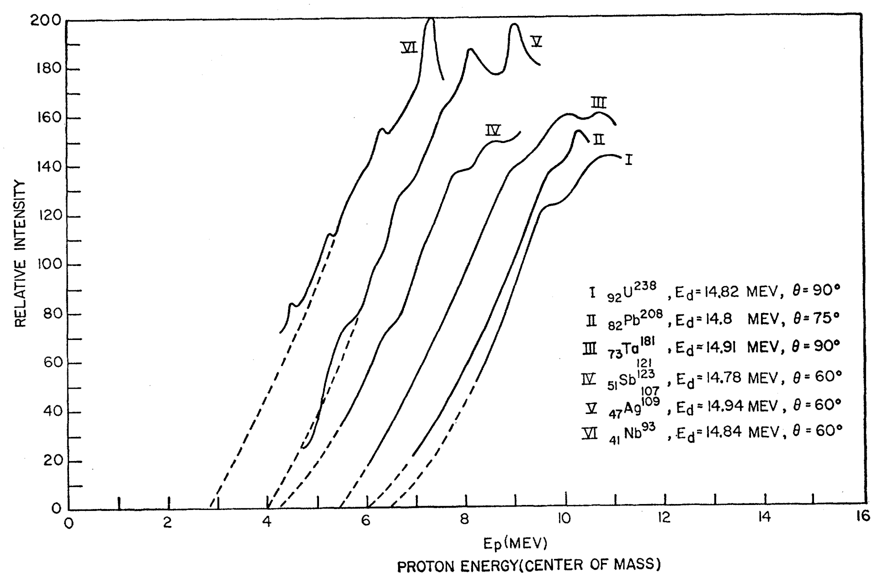

FIG. 11. Variation of low-energy part of proton spectrum with atomic number. Dashed lines obtained by extrapolation.

parent deuteron threshold energy for (d,p) reactions due to the Coulomb barrier. The apparent deuteron threshold energies obtained in this manner have nearly the same values as the apparent experimental cut-off energies in the proton spectra. It, therefore, seems likely that a slight variation of Peaslee's theory can be used to explain the low-energy parts of the proton spectra.

The possibility exists that some of the low-energy protons observed are due to the electric breakup of the deuteron by the Coulomb field of the nucleus. Mullin and Guth calculated cross sections for the electric breakup process.[5] Their calculations indicate that the electric breakup process competes favorably with stripping for targets of Z greater than 29 bombarded by 15-Mev deuterons. Since their calculations do not show the proton energy spectra for the electric breakup, no direct comparison can be made at this time.

To establish definitely what part of the proton spectra observed are due to electric breakup, it will be necessary to determine what happens to the neutrons which are separated from the observed protons. One possible way might be to use a neutron counter in coincidence with the proton counter.

V. ACKNOWLEDGMENTS

The author would like to thank Professor M. S. Livingston under whose direction this work was carried out. His advice and suggestions were very helpful. The author is grateful to Dr. K. Boyer of Los Alamos for suggesting a study of the low-energy protons. He is also grateful to Professor V. Weisskopf and Professor F. Friedman for valuable discussions on the theoretical implications of the results.

Sincerest appreciation is extended to H. S. Stoddart for his design of a large part of the electronic apparatus and for the many suggestions which were extremely helpful in developing the particle selection technique. Appreciation is also extended to Dr. N. S. Wall and J. W. Haffner for their general assistance and helpful suggestions.

The author is indebted to F. Fay, A. Nummela, and E. White of the M. I. T. Cyclotron Crew for their efficient help in the building and maintenance of the experimental apparatus.

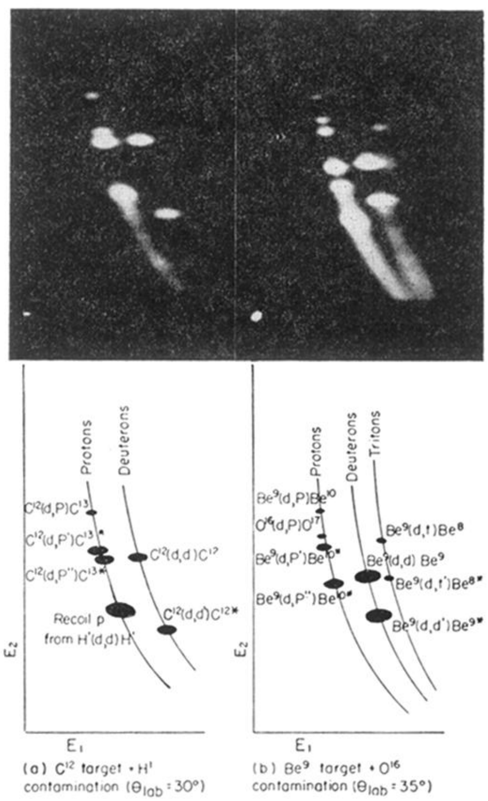

FIG. 2. Time exposure photographs of the oscilloscope screen with the particle selective counter observing reaction particles from 15-Mev deuteron induced reactions. Pulses from the thin plastic scintillation counter (E_1) are displayed on the X-axis and the pulses from the NaI(Tl) counter (E_2) are displayed on the Y-axis. Reprinted in part from M. I. T. Laboratory for Nuclear Science, Progress Report (August 31, 1953).

(a) (b) (c)

FIG. 4. Photograph of oscilloscope screen when counter is observing oxidized Be target at 45 degrees from the incident deuteron beam. Beam energy is approximately 15 Mev. Multiplier output is displayed on X-axis and E_2 is displayed on Y-axis. (a) Analyzers adjusted to count all particles. (b) Product analyzer adjusted to count protons. Some low-energy deuterons are leaking through. (c) Analyzers adjusted to count only protons. This shows the part of the proton spectrum that can be measured with only one adjustment of the product analyzer.

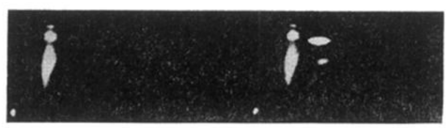

(a) (b)

FIG. 5. Photograph of oscilloscope screen when counter is observing Pb^{206} target bombarded with 15-Mev deuterons. Multiplier output displayed on X-axis, E_2 displayed on Y-axis. Counter angle 90 degrees. (a) Product analyzer adjusted for protons. (b) Analyzers adjusted for all particles.